Blends of Poly(amide-enaminonitrile) with Poly(ethylene oxide), Poly(4-vinylpyridine), and Poly(*N*-vinylpyrrolidone)

J. A. Moore* and Sarjit Kaur‡

Department of Chemistry, Rensselaer Polytechnic Institute, Troy, New York 12180-3590

Received February 4, 1997; Revised Manuscript Received August 13, 1997[⊗]

ABSTRACT: The miscibility behavior of a regularly alternating copoly(amide-enaminonitrile) with several commercial polymers (poly(ethylene oxide) (PEO), poly(4-vinylpyridine) (P4VP), and poly(*N*-vinylpyrrolidone) (PNVP)) was studied by using FTIR spectroscopy and thermal analyses (DSC, TGA, and TMA). Blends of the copolymer with PNVP or P4VP (20−80 wt %) gave transparent films and single glass transition temperatures that changed smoothly with composition, and an enhancement in the thermal stability of the poly(amide-enaminonitrile) component of the blends was observed. With the semicrystalline PEO, miscible blends were obtained at ≤60 wt % PEO. In addition to melting endotherms of PEO crystallites that were observable for ≥40 wt % of PEO samples, the presence of higher temperature endotherms between 140 and 180 °C is consistent with phase separation of the miscible blends (lower critical solution temperatures, LCST). On the time scale of DSC studies, the phase separation of the PEO/copolymer blends is apparently irreversible. When compared to the miscibility behavior of PEO/poly(enaminonitriles) homopolymer blends (based on LCST data, PEO crystallinity, and FTIR carbonyl spectral changes), the interaction of the copolymer with PEO is weaker because of the presence of the amide group. The amide groups apparently prefer to self-associate in the copolymer in preference to interaction with PEO. Similar behavior is also observed for PNVP or P4VP blends with the copolymer.

Introduction

Poly(enaminonitriles) are interesting polymers because they are thermally stable and are soluble in many organic solvents, unlike aramids that show limited solubility. The solubility of poly(enaminonitriles), PEAN, in many organic solvents, such as THF, glymes, pyridines, DMF, NMP, DMAC, and DMSO, has been attributed to the introduction of the rather bulky and polarizable dicyanovinylidene group, in place of oxygen atoms in amide groups, with the apparent consequence of reducing crystallinity and/or very strong hydrogen bonding interactions in the polymers.[1] As a result, unlike the very strongly self-associated amide NH protons in polyamides, the enaminonitrile hydrogen atoms are able to form hydrogen bonds with other proton-accepting functional groups.

In many blend systems, a homogeneous phase is obtained because of the existence of specific interactions between the different polymeric components, which allows mixing on a molecular scale. One such interaction is hydrogen bonding, which has been reported for many polymeric blends.[2] It is evident from the solubility of PEAN in several glyme solvents and the presence of LCST behavior in these solutions that a negative enthalpy of mixing is expected between PEAN and PEO.[1] Polymers containing tertiary amide groups are potentially good proton acceptors because of the basic nature of the functional groups. P4VP is one of the stronger proton acceptors with a basic nitrogen atom at the 4-position of the pyridine ring. The ability of poly(enaminonitrile)s to interact through hydrogen bonding was consequently used to prepare miscible blends with several commercial polymers such as PEO, P4VP, and tertiary amide polymers such as poly(ethyloxazoline), PVNP, and poly(*N*,*N*-dimethylacrylamide). The basis of miscibility in these blends was determined by FTIR spectroscopy to be hydrogen-bonded interactions between the enamine hydrogen atom and electronegative oxygen or nitrogen atoms of the second polymer component.[3]

Regularly alternating aromatic copolymers of amide and enaminonitrile functional groups also exhibit solubility in polar aprotic solvents, THF, pyridine, and diglyme. In this work, the miscibility of a regularly alternating poly(amide-enaminonitrile), copolymer **1**,[4]

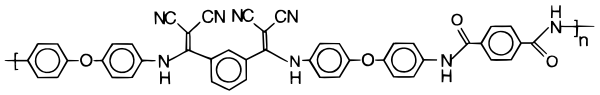

copolymer **1**

with PEO, P4VP, and PNVP was studied to determine (1) if miscibility is retained and (2) if miscibility is retained, does the amide group participate through hydrogen bonding with the other polymer component in the blend?

Results and Discussion

(1) Miscibility Behavior of PEO and Poly(amide-enaminonitrile). The first and second differential scanning calorimograms for films containing 20, 40, 60, and 80 wt % of PEO are shown in Figure 1. The lower temperature endotherms are the melting points of PEO crystallites, and the upper endotherms (140−180 °C) reflect phase separation (LCST) because films are opaque when examined at room temperature after the first run. Earlier results on blends between PEO and poly(enaminonitriles) have similarly reported phase separation in the region of (170−215 °C). While the phase separation was reversible for meta-substituted PEAN homopolymer, it was irreversible for para-

‡ Current address: Department of Chemistry, Vassar College, Poughkeepsie, NY 12601.

[⊗] Abstract published in *Advance ACS Abstracts,* December 15, 1997.

S0024-9297(97)00154-X CCC: $15.00
Published on Web 01/27/1998

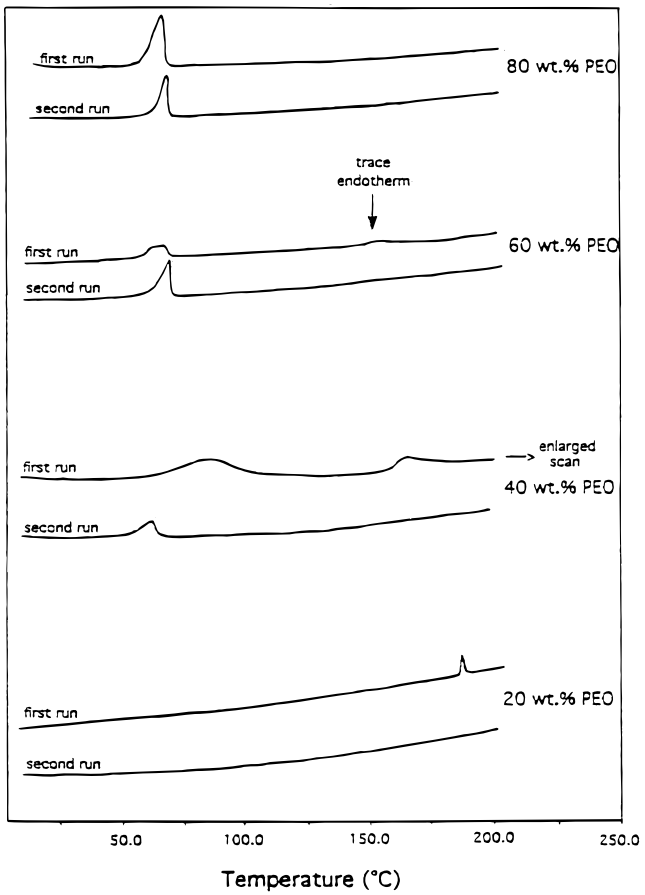

Figure 1. Differential scanning calorimograms of PEO/copolymer **1** blends (top to bottom): (a) 80/20, (b) 60/40, (c) 40/60, and (d) 20/80.

substituted PEAN.[1] On the time scale of the experiment, the phase redissolution of the stiffer, para-linked structure is apparently slower than the crystallization of PEO from the PEO-rich phase during cooling of the phase-separated mixture. The blends of PEO/copolymer **1** also show an apparently irreversible LCST because of sufficient chain rigidity caused by the presence of some para linkages in the copolymer. A further consideration in the case of blends of the copolymer is that redissolution may also be inhibited by re-formation of amide−amide hydrogen bonding.

The thermal properties of PEO/copolymer **1** blends are summarized in Table 1. The percent crystallinity of PEO, X_c, in the blends was calculated using the observed heat of fusion of perfectly crystalline PEO ($H°_{fusion}$) of 213 J/g in the following equation:[5]

$$X_c = (H_{fusion}/H°_{fusion}) \times 100\%$$

The 100% PEO sample melted over a fairly wide range between 58 and 74 °C. Films containing 60 and 80 wt % of PEO were slightly cloudy, and melting endotherms for PEO are observed in the first scan. There is some depression of the melting points of PEO in blends containing 60 and 80 wt % of PEO, which is suggestive of the interaction of PEO in the copolymer. However, these observed melting points are not equilibrium temperatures and the observed depression of the PEO melting points may arise from other causes such as the kinetics of crystallization and morphological factors.[6] Both films containing 60 and 80 wt % of PEO were cloudy when the samples were examined at room temperature after the first runs and melting endotherms of PEO were sharper and shifted to a slightly higher temperature in the second runs. These results are consistent with irreversible phase separations. Another indication of phase separation is the increase in percent crystallinity of the 60 wt % PEO blend (32%) on the second run as compared to the first run (17%). The amount of crystallinity is expected to increase after phase separation because more PEO is available for recrystallization, since it is no longer interacting with the copolymer and, in the absence of miscibility, the copolymer has less of an influence in depressing crystallinity. Additionally, phase separation is also evident in the blend containing 60 wt % PEO from the presence of a small endotherm at 140 °C. In the case of the sample containing 80 wt % PEO, the apparent % crystallinity decreases on the second run and does not indicate phase-separated behavior. The reduced crystallinity is more likely a reflection of the kinetics of crystallization of the PEO component rather than any interaction with the copolymer. The first DSC scan was made on a blend sample annealed at 90 °C for 72 h, which is likely to increase the crystallinity of the pure PEO phase, while the second run was made on a blend sample quenched rapidly to room temperature from a temperature of ∼200 °C. The blend containing 80 wt % PEO is apparently not miscible.

The film containing 40 wt % PEO was transparent but a broad PEO melting endotherm (6% crystallinity) is seen between 66 and 83 °C (peak at 75 °C) on the first run. The PEO melting peak in the blend is as broad as that observed for the 100% PEO sample but, interestingly, is shifted to a slightly higher temperature. This behavior is unexpected and a possible reason for the higher melting temperature range of the PEO crystallites in the blend is that the melting of the PEO crystallites actually occurs prior to the onset of the glass transition temperature (measured at 139 °C by TMA) of the amorphous miscible region. Consequently, the PEO crystallites are melting while the amorphous matrix around the crystallites is in a glassy state. The presence of a glassy matrix may increase and broaden the observed melting range of the PEO crystallites. Phase separation in the blend containing 40 wt % PEO is indicated by an endotherm at 159 °C on the first run, an increase in percent crystallinity on the second run, and cloudiness of the film after the first run. It would appear that the melting of PEO crystallities in the second run is also occurring in a glassy matrix of the amorphous copolymer that has a T_g of 274 °C. However, due to the phase separation taking place at the end the first run, as evidenced by the presence of the endotherm at 140 °C, it is very likely that PEO is not completely crystalline upon cooling and, therefore, the immediate environment of the PEO crystallites is very likely to be amorphous PEO. Thus, the PEO crystallites in the phase-separated sample (second run) are likely to exist in a different matrix environment than the blend sample at the beginning of the first run. PEO crystallites can then be expected to melt in a matrix closer to amorphous PEO on the second run where the immediate amorphous region is above its glass transition temperature. Given this rationale, the PEO melting temperature range for the phase-separated sample (second run) is likely to be closer to or slightly lower than temperatures reported for a 100% PEO sample.

Table 1. Thermal Properties of PEO/Copolymer 1 Blends

	% crystallinity			PEO endotherm (°C)		film appearance		
PEO wt %	1st run	2nd run	T_g[a] (°C)	1st run	2nd run	phase separation[b]	initial	after 1st run
0			274				clear	clear
20			180			184	clear	clear
40	6	14	139	75	57	159	clear	sl cloudy
60	17	32	*c*	56[d]	61	140	hazy	opaque
80	53	28	*c*	53	56	none seen	hazy	opaque
100			−60[6]	58−73 (broad)				

[a] Second runs on TMA reported. [b] Demixing endotherm (LCST) in °C. [c] No T_g seen between −40 and 200 °C. [d] Broad endotherm ranging between 45 and 64 °C.

The blend containing 20 wt % PEO showed phase separation at 184 °C, and no detectable transitions were seen on the second scan. The absence of an endotherm in the LCST region on the second scan shows that the phase separation was irreversible on this time scale in the solid state. A T_g of 180 °C, which is intermediate between those of copolymer **1** and PEO, was measured by TMA.

For the same weight percent PEO, the phase separations in the PEO/copolymer **1** blends occur 25−30 °C lower than those reported for PEO/PEAN homopolymer blends. On the basis of this data and previously reported studies on the lowering of the LCST with decreasing strength of hydrogen bonding,[7] it is concluded that the interaction of PEO with copolymer **1** is weaker than for PEAN homopolymers. Further support for this conclusion is based on the percent crystallinity observed for PEO on the first runs. The rate of crystallization of PEO is lowered to a lesser extent when interacting with copolymer **1** containing carbonyl and dicyanovinylidene functional groups as compared to the homopolymer containing only dicyanovinyl groups. Blends of meta-substituted PEAN/PEO homopolymers show only trace crystallinity at 60 wt % PEO, while crystallinity for blends of PEO/copolymer **1**, on the other hand, persists in blends containing a lower fraction of PEO (i.e. 40 wt % PEO). Crystallization of PEO in blends has been shown to correlate with strengths of interactions between the polymeric components.[7] The greater the interaction between polymeric components, the larger is the inhibiting influence on the PEO crystallization process.

A possible explanation for the observed reduction in hydrogen bond strengths in PEO/copolymer **1** blends may relate to the available hydrogen bonding sites between the two polymeric components. Both carbonyl and nitrile groups are known to interact through hydrogen bonding, but the oxygen atom of the carbonyl group is expected to be a better electron donor and its intermolecular interactions through hydrogen bonding are likely to be stronger than the lone pairs of the sp-hybridized nitrogen atom of the nitrile groups. A possible outcome of the difference in the strengths of interactions of the nitrile groups and carbonyl groups is that PEO may be able to compete with the nitrile groups for the available acidic protons but is unable to break the stronger hydrogen-bonded associations of the carbonyl groups. Therefore, the interacting sites for blending with PEO are potentially reduced by half in the copolymer as compared to PEAN homopolymers. The weaker interaction of PEO with the copolymer is speculated at this point to be a consequence of a reduction in the number of interacting sites.

The existence of hydrogen-bonded interactions in the PEO/copolymer blends was studied by FTIR spectroscopy (Figure 2). A physical mixture was prepared from weighed polymers that were ground together with KBr for 1 min to obtain a pellet. The NH region of the infrared spectrum of the copolymer is broad because of the different types of bonded and nonbonded states of both enamino and amide groups, making it difficult to monitor any changes in this region. However, hydrogen-bonded interactions of PEAN homopolymers with PEO have been established by observation of shifts in the NH region to lower frequency (from 3255 to 3230 cm^{-1}).[1,3] Therefore, the enaminonitrile proton in the copolymer is expected to interact with PEO through hydrogen-bonding interactions.

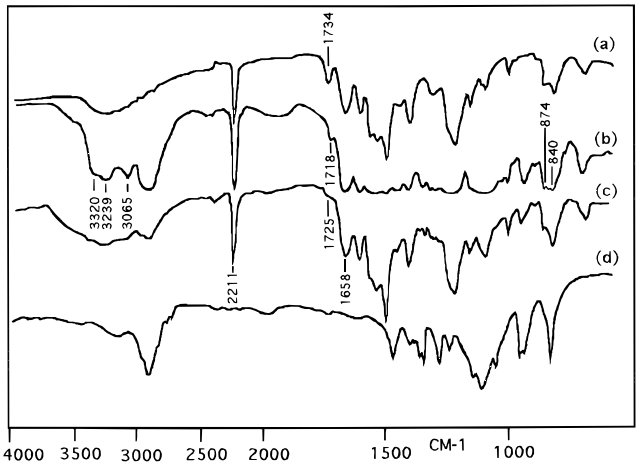

Figure 2. FTIR spectra: (a) copolymer **1**; (b) 40/60 wt % PEO/copolymer **1** blend; (c) physical mixture of 40/60 wt % PEO/copolymer **1**; (d) PEO.

While qualitative interpretations of FTIR spectra between the blend sample (film) and "physical mixture" sample (KBr pellet) may potentially be problematic due to possible interaction of K^+ with the carbonyl oxygen atom and bromide with NH in the latter case, the FTIR data for the blend film sample can be evaluated against results for the copolymer film. Although there are no definitive shifts in a single peak, the broad band seen for the NH stretching region in the copolymer is shaping into two bands in the 40 wt % PEO blend, and the intensity of the band at 3239 cm^{-1} is greater than the band at 3320 cm^{-1}. These results can be interpreted as changes in hydrogen-bonded interactions in the blend sample. The lack of a specific shift of a band in the NH stretching region may not be surprising because of the possibility that the hydrogen-bond strengths may not change significantly from the copolymer to the blend samples. The absence of a clear cut shift in the N−H stretching region to reflect hydrogen-bonded interactions has also been previously noted for an amorphous poly(urethane−ether) blend.[8] The FTIR spectrum of the copolymer shows a "free" carbonyl band at 1734 cm^{-1}.

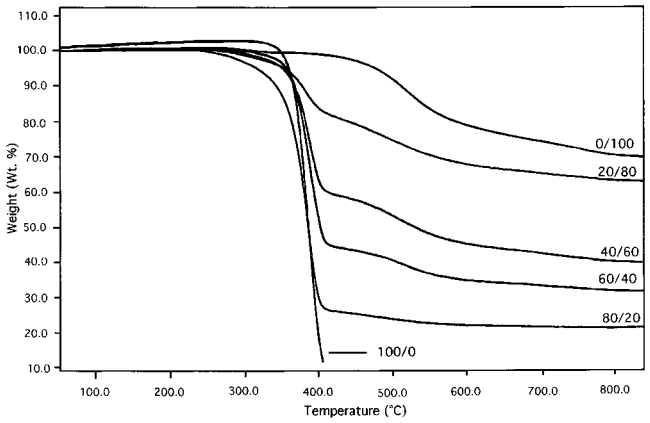

Figure 3. Thermogravimograms in nitrogen of PEO/copolymer **1** Blends.

Of interest is the apparent shift of the "free" carbonyl band to lower frequency in the blend containing 40 wt % PEO relative to the physically mixed sample and to copolymer **1**. This shift to lower frequency suggests hydrogen bonding at the amide group and, given that the PEO is not a proton donor, the carbonyl oxygen atom is most likely associated with the amide or enaminonitrile proton of the copolymer, and consequently, the number of amide/enaminonitrile protons available for hydrogen bonding with the oxygen atom of PEO is reduced. This reasoning is in agreement with the previous suggestion of reduced interaction of the copolymer with PEO. Another region of the IR spectrum that has been correlated with hydrogen bonding is the amide V region (700 cm^{-1}).[2d] This region contains significant contributions from N−H out-of-plane deformations. With increasing temperatures, the intensity of the amide V band for aliphatic polyamides decreases with reduction of the hydrogen-bonded interactions in the polymer, while an absorption band nearby remained unchanged.

The FTIR spectrum for the blend sample of PEO/copolymer shows that there are two peaks near the amide V band region, namely 840 and 874 cm^{-1}, and the band at 840 cm^{-1} shows different intensities in the blend and physically mixed samples. The band at 874 cm^{-1} is assigned to the amide V band for the copolymer because comparison with other aromatic polyamides shows this band to be present between 865 and 870 cm^{-1}.[1b] For Kevlar, the amide V band was assigned to 865 cm^{-1}.[9] PEAN homopolymers showed a band consistently between 835 and 840 cm^{-1}, and therefore, the band at 840 cm^{-1} for the copolymer is tentatively assigned to enaminonitrile protons (out-of-plane NH deformation mode). In the blend samples, there are overlapping bands at 840 cm^{-1}, contributions from both the copolymer and PEO). As shown in Figure 2, the intensity of the band at 840 cm^{-1} of the blend sample is reduced when compared to the physically mixed sample. With PEO competing for the NH sites of the enaminonitriles in the blends, the internal hydrogen-bonded network of enaminonitriles is expected to decrease. This change may possibly be reflected in the lowered intensity of the band at 840 cm^{-1}.

The thermogravimetric scans in nitrogen of PEO/copolymer blends are shown in Figure 3. The blends show two decomposition onsets. The degradation step at about 470 °C is broad and corresponds to the copolymer **1** component. The first onset of degradation coincides with PEO degradation, at about 350 °C. There

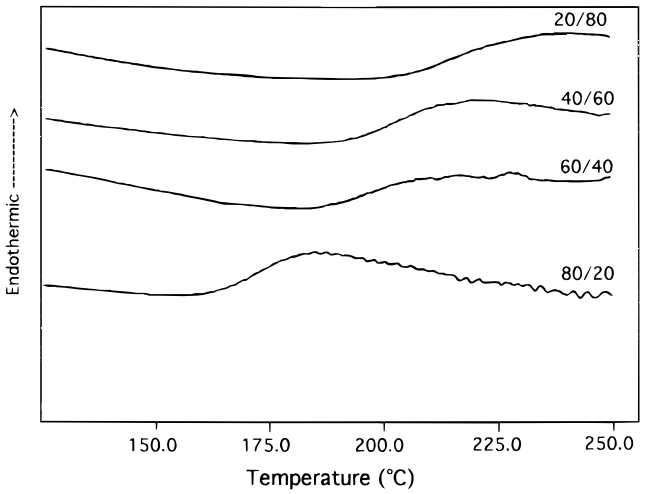

Figure 4. Differential scanning calorimograms of P4VP/copolymer **1** Blends.

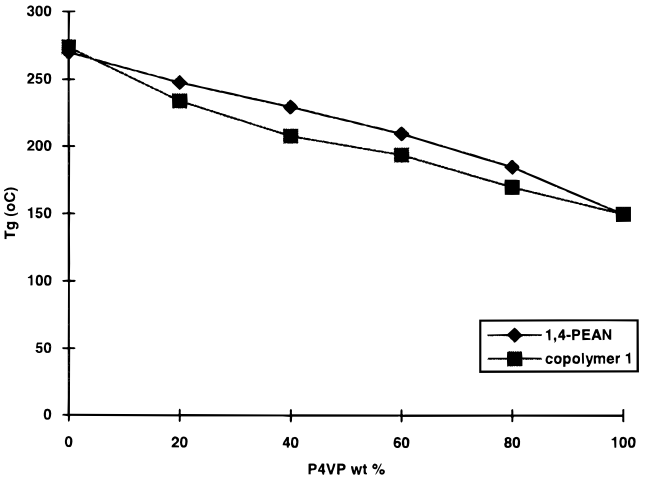

Figure 5. T_g vs composition curve of P4VP/copolymer **1** and P4VP/1,4-PEAN blends.

is a slight improvement in the thermal stability of the PEO component for the blend containing 20 wt % PEO, while a slight reduction in thermal stability is observed for the sample containing 80 wt % PEO. The blends containing 40 and 60 wt % PEO show comparable thermal stability to pure PEO.

(2) Miscible Blends of Poly(4-vinylpyridine)/Copolymer 1. The films obtained were yellow but transparent. The T_g values of the films were between the values of P4VP and copolymer **1**, and a steady increase in T_g was observed as the copolymer content increased (Figure 4). Shown in Figure 5 is the variation of T_g values with blend composition for P4VP/copolymer **1** and previously reported data of P4VP/1,4-substituted homopoly(enaminonitriles)[3]. The T_g values of the blends with copolymer **1** are consistently lower than those reported for the corresponding blends with 1,4-PEAN homopolymer.

Hydrogen bonding in blends of homopolymers 1,4-PEAN and P4VP was previously established by FTIR and NMR study of a mixture of a model compound, 1,3-bis[2,2-dicyano-1-(4-phenoxyphenyl)aminovinyl]-benzene, with pyridine.[3] Similar hydrogen-bonding interactions were expected to be observed for blends of P4VP/copolymer **1** by FTIR spectroscopy but, as shown in Figure 5, the N−H region of copolymer **1** is broad and it is difficult to monitor specific band shifts.

However, there are some indications of changes in hydrogen-bonding patterns of the amide/enaminonitrile protons when the NH region of the FTIR spectrum of the blend sample of 40 wt % P4VP is compared to that of the physically mixed sample. The NH region of the blend sample is not as broad and the bands are more defined, indicative of changes in hydrogen bonding. The presence of the band at 3065 cm^{-1}, however, has been reported as more likely an overtone of the amide II band;[10] it also appears in the physically mixed sample. Because of the difficulty in characterizing intermolecular hydrogen-bonded interactions, model compound **2**

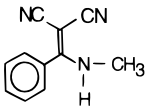

2

was used to form hydrogen-bonded complexes with proton acceptors (see next section). The existence of a hydrogen-bonded complex of model compound **2** with *trans*-1,2-bis(4-pyridyl)ethylene (BPE) establishes that the miscible behavior of blends of P4VP and copolymer **1** is the consequence of hydrogen bonding between the nitrogen atoms of the pyridine rings in P4VP and enaminonitrile/amide protons.

As reported for PEO/copolymer **1** blends, and seen more clearly here for blends of P4VP/copolymer **1**, the "free" carbonyl band seen at 1734 cm^{-1} for copolymer **1** is not evident in the blend of 40 wt % P4VP. The "free" carbonyl band is possibly shifted to lower frequencies and found in the overlapping region of ~1660 cm^{-1}. The 1734 cm^{-1} band is present in the physically mixed sample, which represents a mixture and not a miscible blend. The shift to lower frequency in the blend sample indicates hydrogen bonding at the carbonyl group, and the same correlation is drawn as discussed earlier for PEO/copolymer **1** blends. As a result of hydrogen bonding at the carbonyl group, the number of available enaminonitrile/amide protons for interaction with P4VP is probably reduced.

Another region of the FTIR spectrum that shows possible hydrogen bonding is the band at 835 cm^{-1}. The intensity of the band at 835 cm^{-1} for the blend sample is observed to be reduced, relative to the physically mixed sample (Figure 6), and correlates possibly with reduced hydrogen bonding among the enaminonitrile groups of copolymer **1**, similar to the observations made for PEO/copolymer **1** blends based on FTIR spectral data. The decrease in the intensity of the band at 835 cm^{-1} is consistent, because as the NH groups of enaminonitriles interact with P4VP, the internal network of enaminonitrile hydrogen bonding is expected to be reduced.

The thermal stability in air of P4VP/copolymer **1** blends is shown in Figure 7. There are two onsets of degradation observed in the regions of 300−350 °C and ~500−550 °C. The first one, corresponding to the P4VP component of the blends, was lower than for 100% P4VP in air. Clearly, the thermal stability of P4VP in the blends is reduced through interactions with copolymer **1**. The second degradation onset corresponds to the copolymer **1** component, and an improvement in thermal stability of 30−45 °C relative to copolymer **1** is evident. Similar patterns in thermal stabilities were reported for blends of P4VP and meta-substituted PEAN.[3] One possible reason for the enhancement of the thermal

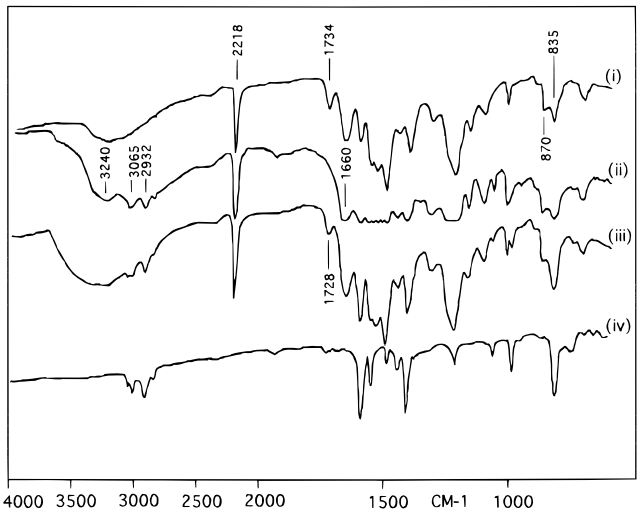

Figure 6. FTIR spectra of (i) copolymer **1**, (ii) blend of 40/60 wt % P4VP/copolymer **1**, (iii) physical mixture of 40/60 wt % P4VP/copolymer **1**, and (iv) P4VP.

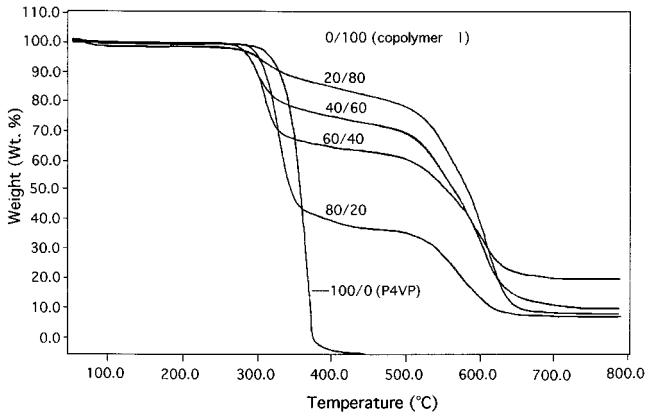

Figure 7. Thermogravimograms in air of P4VP/Copolymer **1** blends.

stability of the copolymer **1** component in the blends is that the P4VP may act as a scavenger for any residual acidic byproducts that may have remained in the polymer. HCl is generated during polymerization, and although acid acceptors are used in the polymerizations, some may remain in the polymers. During heating of the copolymer, residual acid may initiate degradation of the polymers at elevated temperatures.

(3) Hydrogen-Bonded Complexes of Model Compounds. To substantiate further the existence of hydrogen bonding between poly(enaminonitriles) and proton-accepting groups, the interaction of model compound **2** was studied with quinone, acetone, triphenylphosphine oxide (TPPO), and *trans*-1,2-bis(4-pyridyl)-ethylene (BPE). Three methods were used to obtain molecular complexes for model compound **2**. The first was crystallization from ethyl acetate (except for acetone, which was used alone). The second and third methods were physical grinding of the solid mixtures for 5 min and crystallization from a mixed melt, respectively. The results of the melting point measurements and infrared spectra of the crystals obtained are reported in Table 2. The crystals from acetone and quinone gave no indication of formation of a molecular complex; **2** was recovered with melting points close to crystals of pure **2** from ethyl acetate. The samples from **2** and TPPO gave broad melting regions between 110 and 130 °C, but no changes in the NH region of the

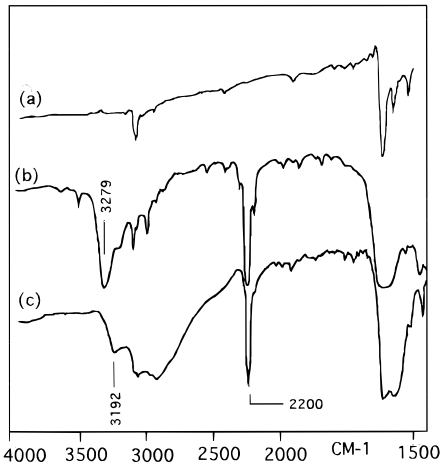

Figure 8. FTIR spectra of (a) *trans*-1,2-bis(4-pyridyl)ethylene (BPE), (b) model compound **2**, and (c) crystals obtained from crystallization of a solution of BPE and model compound **2** in ethyl acetate.

Table 2. Melting Points and Infrared N−H Shifts of Crystals Obtained from Mixtures of Model Compound 2 and Proton Acceptors

proton acceptor used with model compound **2**	melting point of crystals obtained from mixture of **2** and acid acceptor, °C	N−H IR stretching region of crystals obtained form mixture of **2** and acid acceptor, cm^{-1}
ethyl acetate (as solvent)	192	3279
TPPO, from solution	110−130, broad	3270
TPPO, ground	113, broad	3279
TPPO, melted	120, broad	3250
BPE, from solution	138	3192
BPE, ground	136	3196
BPE, melted	136	3190
acetone (as solvent)	192	3278
quinone, from solution	193	3280

infrared spectra were observed. The lowering of the melting points is most likely due to the formation of eutectic mixtures. The melting points of BPE and **2** are 192 and 153 °C, respectively. A melting point of 138 °C was measured for crystals obtained from an ethyl acetate solution of BPE and **2**. The occurrence of hydrogen bonding in the crystal was observed by a shift to a lower frequency of 3192 cm^{-1}, relative to the N−H band at 3279 cm^{-1} for **2** (see Figure 8). The existence of hydrogen bonding is further supported by ^1H NMR data where a broad band at 9.6 ppm (NH) is observed for the crystals melting at 138 °C, which is a downfield shift from 8.0 ppm observed for the NH resonance of pure **2**. The hydrogen-bonding interaction is most likely between the enaminonitrile proton and the basic nitrogen atom of the pyridine ring in BPE. Crystals melting at 138 °C and showing hydrogen-bonded interactions (as observed by infrared spectroscopy) could also be prepared by physical grinding and crystallization from a mixed melt.

(4) Miscible Blends of Poly(*N*-vinylpyrrolidone)/copolymer 1. Films of PNVP/copolymer **1** were yellow but clear and gave single T_g values that are intermediate between copolymer **1** and PNVP, indicating miscibility of the blends. The T_g values of the blends varied smoothly with increasing composition of copolymer **1** (Figure 9). A comparison of the T_g values of PNVP/copolymer **1** and PNVP/1,3-PEAN homopolymer[3] (Figure 10) shows that the T_g values of the blends with copolymer **1** are consistently lower than the corresponding weight percent blends with PEAN homopolymer. The same result was also observed for blends with P4VP.

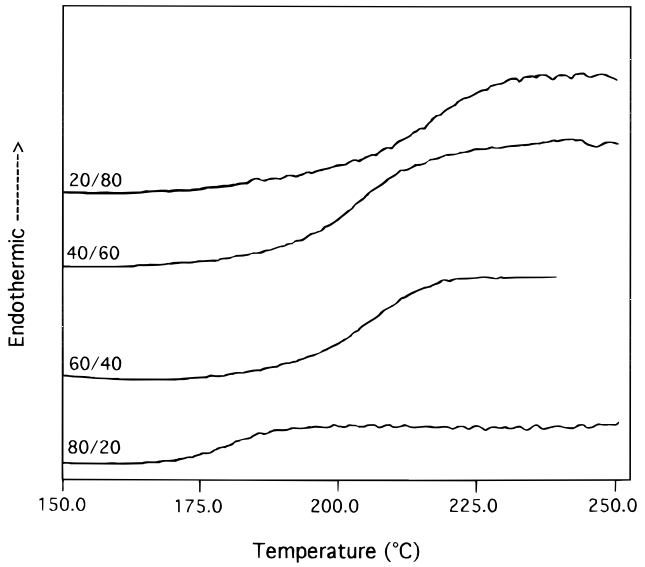

Figure 9. Differential Scanning Calorimograms of PNVP/Copolymer 1 Blends.

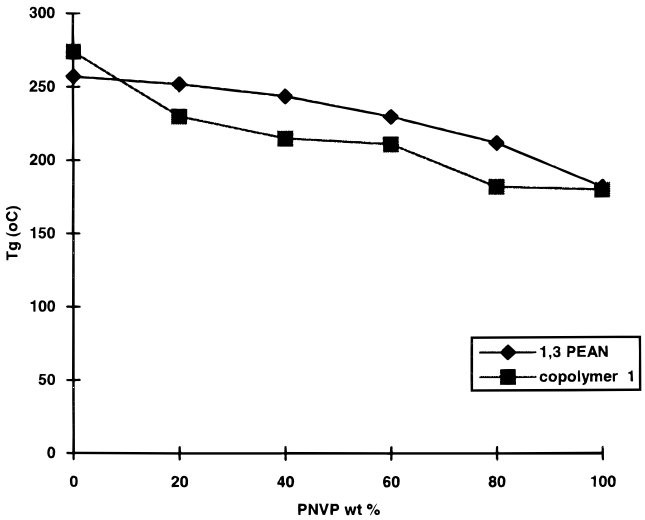

Figure 10. T_g vs composition curve of PNVP/copolymer **1** and PNVP/1,3-PEAN blends.

The TGA traces for PNVP/copolymer **1** blends studied in air are shown in Figure 11. The copolymer **1** component in the blends shows a definite improvement in thermal stability by as much as 50−70 °C relative to pure copolymer **1**. This trend was also observed for P4VP/copolymer blends. The thermal stability of PNVP component in the blends appears unchanged relative to pure PNVP, except that the blend containing 40 wt % PNVP shows an earlier degradation onset. Thermal stabilities measured in nitrogen also showed neglible changes in the thermal stability of the PNVP in the blends.

The evaluation of hydrogen-bonded interactions using FTIR spectroscopy for PNVP/copolymer **1** blends suffers from the same drawbacks as reported for P4VP/copolymer **1** blends. As shown in Figure 12, the general broadness of the NH region and overlapping peaks in the amide region pose difficulties in monitoring defini-

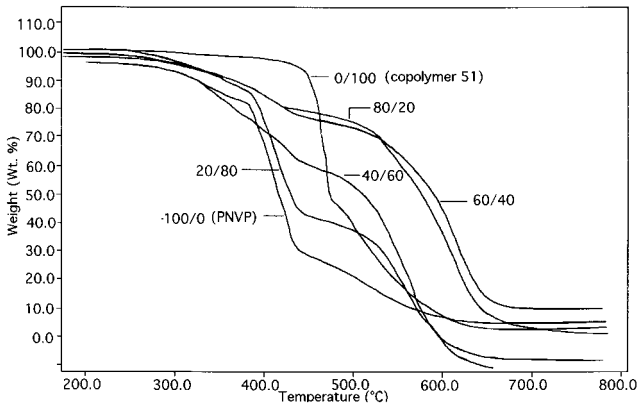

Figure 11. Thermogravimograms in air of PNVP/copolymer **1** blends.

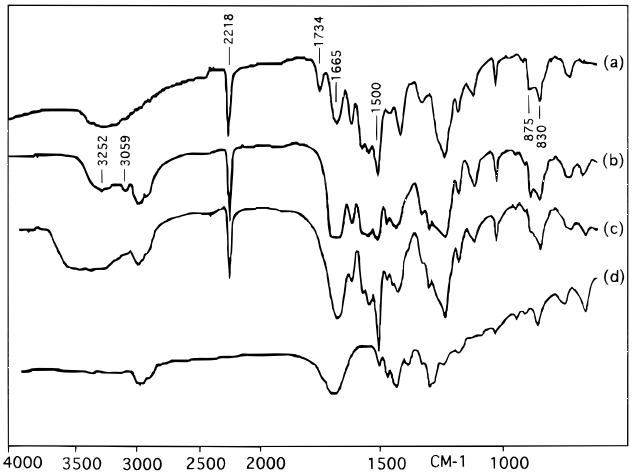

Figure 12. FTIR spectra of (a) copolymer **1**, (b) blend of 40/60 wt % of PNVP/copolymer **1**, (c) physical mixture of 40/60 wt % of PNVP/copolymer **1** and (d) PNVP.

tive shifts in the desired bands. No shift in any peak is observable in the NH region, other than the presence of the peak at 3059 cm^{-1}, which is most likely an overtone band of amide II. The "free' carbonyl band seen at 1730 cm^{-1} in copolymer **1** is again not seen in the blend sample, and is possibly shifted to lower frequency. The 1730 cm^{-1} band of the physical mixture is present as a shoulder on the broad and symmetrical carbonyl band of PNVP. The shift of the "free" carbonyl band to lower frequency in the blends is possibly correlated with increasing hydrogen-bonding interactions at the amide group of copolymer **1**. Another region of the FTIR spectrum that warrants attention is the decrease in intensity of the 830 cm^{-1} band in the blend samples, relative to the physical mixture, which is suggestive of reduced hydrogen bonding of the enaminonitrile groups of copolymer **1** as a consequence of the interaction of the enaminonitrile proton with PNVP.

Conclusions

An aromatic copolymer containing amide and enaminonitrile groups gave miscible blends with PEO (up to 60 wt % PEO), PNVP, and P4VP polymers. The basis for the miscibility is most likely hydrogen-bonding interactions between the enaminonitrile proton and proton-accepting sites of PEO, PNVP, and P4VP. The strength of the hydrogen-bonding interactions observed for blends of the copolymer are different than those for PEAN because blends of the copolymers exhibited lower LCST values, by as much as ~30 °C, than corresponding wt % PEAN/PEO homopolymer blends. Additionally, T_g values of the blends for the copolymer with PNVP and P4VP are consistently lower than the corresponding blends with PEAN homopolymer. These results indicate that the hydrogen-bonded interactions that contribute to the miscibility of the copolymer blends are decreased. A possible explanation for the decrease in hydrogen-bonded interactions of the copolymer blends may relate to the observation of hydrogen-bonded interactions at the carbonyl group of the copolymer in the blend samples. On the basis of FTIR spectral data, the frequency of the copolymer carbonyl absorption in the blend samples is shifted to lower frequency than a sample containing 100 wt % copolymer **1**. Because the copolymer is the only source of acidic protons in the blends, the hydrogen-bonded interactions observed at the carbonyl group must arise from the interaction of acidic protons of the copolymer with the basic oxygen atom of the carbonyl group in the copolymer, thus reducing proton-donating sites of the copolymer in the blend samples for interaction with proton-accepting sites of PEO, PNVP, and P4VP. Consequently, the number of hydrogen-bonding sites available for establishing miscibility in the copolymer are reduced by half compared to those of the PEAN homopolymer and is a possible explanation for the general observation of weaker hydrogen-bonded interactions in blends with the copolymer than with PEAN homopolymers.

Experimental Section

Materials. Copolymer **1**[4] had an intrinsic viscosity of 0.62 dL/g in DMF at 25.00 °C, as measured with a Cannon-Ubbelohde viscometer. A M_W of 56 900 and a polydispersity of 2.1 was determined by GPC, relative to PEO standards using 0.1 M $LiNO_3$ in DMF as solvent. A set of three microStyragel columns (10^3, 10^4, 10^5) in series were used at a flow rate of 0.8 mL/min. PEO and PNVP were purchased from Aldrich Chemical Co. with average molecular weights of 1×10^5 and 4×10^4, respectively. P4VP was obtained from Polysciences, Inc. with a molecular weight of 5×10^4. The polymers were used as received without further purification. HPLC grade DMF was used to prepare solutions of the blends.

Blend Preparations. The blend solutions were prepared by dissolving a total weight of 0.100 g of the polymers in 5−7 mL of DMF. A series of blend compositions containing 0, 20, 40, 60, 80, and 100% of copolymer **1** (wt/wt) were prepared for each blend study. The solutions were filtered through a fine fritted glass filter funnel and placed in aluminum pans. DMF was evaporated slowly in vacuo (2−3 Torr) at room temperature for 18 h, and the films were dried further at 90 °C for 72 h in vacuo (1−2 Torr). The films were stored in a desiccator prior to measurement. Despite the vacuum drying, a small amount of DMF remained in the samples. Measurements of the films by TGA indicated the presence of some residual solvent, ranging between 2 and 5% for blends of P4VP and PNVP.

Instrumentation. Calorimetric measurements were made under nitrogen on a Perkin-Elmer System 7 differential scanning calorimeter interfaced with a Perkin-Elmer Model 7500 computer. Sample sizes ranged between 5 and 10 mg and samples were encapsulated in aluminum pans. An empty aluminum pan was used as a reference. Samples were heated at 10 or 20 °C/min, and the midpoint of the heat capacity change was taken as the glass transition temperature. Residual solvent in the films was removed once the films were heated through the glass transition temperatures, and consequently, the T_g from the second heating cycle was reported. The T_g values were also measured by thermal mechanical analysis (TMA) when a cohesive film was available. TMA was performed on a Perkin-Elmer TMA7 instrument interfaced

with an IBM PS/2 Model 55 SX computer. An extension probe with 200−250 mN of applied force was used to measure the T_g values of films. The analysis was carried out under helium between 100 and 300 °C at a heating rate of 10 °C/min. The glass transition temperatures were reported as the inflection point of the second or third runs. FTIR spectra were recorded on a Perkin-Elmer Model 1800 spectrometer at a resolution of 2 cm^{-1}. At least 32 scans were signal-averaged. NMR spectra were recorded on a Varian Model XL-500 spectrometer.

Synthesis of 2,2-Dicyano-1-(*N*-methylamino)vinylbenzene (2). Methylamine HCl (1.77 g, 21.3 mmol), DMAP (4.767 g, 42.6 mmol), and 25 mL of anhydrous DMAC were placed in a dried 300 mL three-necked flask, equipped with a nitrogen inlet, magnetic stirrer, and water-cooled condenser. 1-Chloro-2,2-dicyanovinylbenzene[1a,11] (4.000 g, 21.3 mmol) was added slowly as a solid, and a cloudy yellow solution was obtained. The reaction mixture was stirred at room temperature for 2 h, followed by heating between 70 and 75 °C for 3 h, and precipitated with water upon cooling of the reaction mixture to room temperature. A light lavender solid was obtained, which was dried in vacuo (2−3 torr) at 40 °C for 48 h over P_2O_5 (3.23 g, 83.0%). The crude product was purified by recrystallization from ethyl acetate (1.2 g, 31%), mp 192−194 °C (DSC) (lit.[12] 189 °C). ^{1}H NMR (acetone-d_6): ppm [2.87, 3.39] (two sets of doublets, 3H, CH_3), 7.40−7.70 (m, 5H, aromatic protons), 7.90 (br, s, 1H, NH).

Acknowledgment. This work was supported partially by a grant from the Office of Naval Research.

References and Notes

(1) (a) Moore, J. A.; Robello, D. R. *Macromolecules* **1989**, 22, 1084. (b) Kim, J. H. Ph.D. Dissertation, Rensselaer Polytechnic Insitute, 1991.

(2) (a) Coleman, M. M.; Moskala, E. J. *Polymer* **1983**, *24*, 251. (b) Coleman, M. M.; Moskala, E. J.; Howe, S. E.; Painter, P. C. *Macromolecules* **1984**, *17*, 2217. (c) Coleman, M. M.; Skrovanel, D. J. Hu, J.; Painter, P. C. *Macromolecules* **1988**, *21*, 2221. (d) Coleman, M. M.: Lee, J. Y.; Painter, P. C, *Macromolecules* **1988**, *21*, 346. (e) Coleman, M. M.; Lee, J. Y.; Painter, P. C, *Macromolecules* **1988**, *21*, 954. (f) Smith, K. L.; Winslow, A. E.; Petersen, D. E. *Ind. Eng. Chem.* **1959**, *51*, 1361.

(3) (a) Moore, J. A.; Kim, J. H. *Macromolecules* **1992**, *25*, 1427. (b) Moore, J. A.; Kim, J. H.; Seidel, P. R. *Chem. Mater.* **1991**, *3* (4), 742.

(4) Moore, J.; Kaur, S. *Macromolecules* **1997**, *30*, 3427.

(5) Li, X.; Hsu, S. L. *J. Polym. Sci., Polym. Phys. Ed.* **1984**, *22*, 1331.

(6) (a) Wang, T. T.; Nishi, T. *Macromolecules* **1975**, *8*, 909. (b) Runt, J. P.; Rim, P. B. *Macromolecules* **1984**, *17*, 1520. (c) Russell, T. P.; Alfonso, G. C. *Macromolecules* **1986**, *19*, 1143.

(7) (a) Ellis, T. S. *Polymer* **1988**, *29*, 2015. (b) Ellis, T. S. *Macromolecules* **1989**, *22*, 742. (c) Kwei, T. K.; Pearce, E. M.; Min, B. Y. *Macromolecules* **1985**, *18*, 2326.

(8) Coleman, M. M.; Skrovanek, D. J.; Hu, J.; Painter, P. C. *Macromolecules* **1988**, *21*, 59.

(9) Mosquera, M. E. G.; Jamond, M; Alonso, A. M. Tascon, J. M. D. *Chem. Mater.* **1994**, *6*, 1918.

(10) Garcia, D.; Starkweather, W. H. *J. Polym. Sci., Polym. Phys. Ed.* **1985**, *23*, 537.

(11) Moore, J. A.; Robello, D. R. *Macromolecules* **1986**, *19*, 2667.

(12) Nakao, H.; Soma, N; Sunagawa, G. *Chem. Pharm. Bull.* **1965**, *13* (7), 828; *Chem. Abstr.* **1965**, *63*, 13141.

MA9701548